Interaction Notes
Note 43

August 1969

Some Theoretical-Numerical Procedures for the Study of the Two-Dimensional Scattering from Arbitrary Shapes

by

Thomas H. Shumpert
Mississippi State University
State College, Mississippi

ABSTRACT

In this note the formulation of the two-dimensional scattering problem is presented. The scattered objects are a discontinuous-radius cylinder, a cone, and a sphere. To determine the scattered fields, Maxwell's equations are solved directly by the use of a finite difference technique. Theoretical results are presented and discussed.

INTRODUCTION

Recently it was shown that finite difference techniques may be used to solve Maxwell's equations directly for an electromagnetic pulse propagation and scattering in time-varying, inhomogeneous media (1). By extending those techniques, it is shown that two-dimensional scattering from arbitrarily curved surfaces also may be treated. The finite difference scheme requires the incident fields to be continuous functions of position and to be two-dimensional. Otherwise, there are no restrictions on the incident pulse. This study has application to radar pulse propagation and scattering in the vicinity of fireballs from nuclear explosions and the wakes of high speed re-entry vehicles. To illustrate the techniques the incident pulse is considered to be propagating in a cylinderical waveguide; the scatterer is considered to be located on the axis of the waveguide, and the axis of symmetry of the scatterer is coincident with the axis of the waveguide. The scattering objects considered are a discontinuous-radius cylinder, a cone and a sphere.

1 System of Partial Differential Equations

Consider an isotropic medium where the relations

$$\vec{B}(\vec{r},t) = \mu_o \vec{H}(\vec{r},t) \tag{1.1}$$

$$\vec{D}(\vec{r},t) = \varepsilon \vec{E}(\vec{r},t) \tag{1.2}$$

$$\vec{J}(\vec{r},t) = \sigma(\vec{r},t)\ \vec{E}(\vec{r},t) \tag{1.3}$$

are satisfied. (The notation is consistent with Jones' text (2).) From Maxwell's equations we have

$$\text{curl}\ \vec{H}(\vec{r},t) = \vec{J}(\vec{r},t) + \frac{\partial}{\partial t}\vec{D}(\vec{r},t) \tag{1.4}$$

$$\text{curl}\ \vec{E}(\vec{r},t) = -\frac{\partial}{\partial t}\vec{B}(\vec{r},t) \tag{1.5}$$

$$\text{Div}\ \vec{D}(\vec{r},t) = \rho \tag{1.6}$$

$$\text{Div}\ \vec{B}(\vec{r},t) = 0 \tag{1.7}$$

Equations (1.1) - (1.5) are sufficient to determine the electromagnetic field. If these equations are expanded in cylindrical coordinates with aximuthal symmetry they produce the three partial differential equations shown below

$$\varepsilon(z,r,t)\frac{\partial}{\partial t}E_r(z,r,t) = -\frac{\partial}{\partial z}H_\phi(z,r,t) - \sigma_e(z,r,t)\ E_r(z,r,t) \tag{1.8}$$

$$\varepsilon(z,r,t)\frac{\partial}{\partial t}E_z(z,r,t) = \frac{1}{r}\frac{\partial}{\partial r}rH_\phi(z,r,t) - \sigma_e(z,r,t)\ E_z(z,r,t) \tag{1.9}$$

$$\mu_o\frac{\partial}{\partial t}H_\phi(z,r,t) = \frac{\partial}{\partial r}E_z(z,r,t) - \frac{\partial}{\partial z}E_r(z,r,t) \tag{1.10}$$

where r, ϕ, and z are the usual cylindrical coordinates and

$$\sigma_e(z,r,t) = \sigma(z,r,t) + \frac{\partial}{\partial t}\ \varepsilon(z,r,t) \tag{1.11}$$

Hence equations (1.8) - (1.10) is the system of equations which must be solved to obtain the electromagnetic fields.

2 Corresponding Finite Difference Equations

The system of partial differential equations obtained in Sec. 1 yields to a solution by finite difference techniques. The method used to set up the difference equations is one given by Lax (3). This method automatically "centers" the difference formulas and hence reduces truncation error. Applying this method to the system of partial differential equations gives the resulting equations

$$H_\phi^{N+1}(I,J) = H_\phi^{N}(I,J) + \frac{1}{\eta}\frac{\Delta\tau}{\Delta r}\left[E_z^{N+\frac{1}{2}}(I,J+\tfrac{1}{2}) - E_z^{N+\frac{1}{2}}(I,J-\tfrac{1}{2})\right] - \frac{1}{\eta}\frac{\Delta\tau}{\Delta z}\left[E_r^{N+\frac{1}{2}}(I+\tfrac{1}{2},J) - E_r^{N+\frac{1}{2}}(I-\tfrac{1}{2},J)\right] \tag{2.1}$$

$$E_z^{N+3/2}(I,J+\tfrac{1}{2}) = E_z^{N+\frac{1}{2}}(I,J+\tfrac{1}{2}) + \eta\left\{\frac{\Delta\tau}{\Delta r}H_\phi^{N+1}(I,J+\tfrac{1}{2})/J + \frac{\Delta\tau}{\Delta r}\left[H_\phi^{N+1}(I,J+1) - H_\phi^{N+1}(I,J)\right] - \Delta\tau\,\sigma_e^{N+1}(I,J+\tfrac{1}{2})\,E_z^{N+1}(I,J+\tfrac{1}{2})\right\}/\varepsilon_r^{N+1}(I,J+\tfrac{1}{2}) \tag{2.2}$$

$$E_r^{N+3/2}(I+\tfrac{1}{2},J) = E_r^{N+\frac{1}{2}}(I+\tfrac{1}{2},J) - \eta\left\{\frac{\Delta\tau}{\Delta z}\left[H_\phi^{N+1}(I+1,J) - H_\phi^{N+1}(I,J)\right] + \Delta\tau\,\sigma_e^{N+1}(I+\tfrac{1}{2},J)\,E_r^{N+1}(I+\tfrac{1}{2},J)\right\}/\varepsilon_r^{N+1}(I+\tfrac{1}{2},J) \tag{2.3}$$

where the following notation is used

$\tau = ct$, $c = \dfrac{1}{\sqrt{\mu_o\varepsilon_o}}$ is the speed of light in free space

$\eta = \sqrt{\dfrac{\mu_o}{\varepsilon_o}} \simeq 120\pi$ ohms

$$\left[H_\phi(z,r,t)\right]_{\substack{z = I\Delta z \\ r = (J-\frac{1}{2})\Delta r \\ t = N\Delta\tau/c}} = H_\phi^{N}(I,J)$$

and ε_r is the relative permittivity, i.e.,

$$\varepsilon(z,r,t) = \varepsilon_0 \varepsilon_r(z,r,t)$$

which may be a function of both time and position.

A close look at the arguments for any given field component reveals that indices are not necessarily consistent. These inconsistencies must be removed before the solution can be effected. Removal may be accomplished in the following manner: Notice that the magnetic field component H_ϕ is evaluated at $r = (J - \frac{1}{2})\Delta r$ in (2.1) and at $r = J\Delta r$ in (2.2) . Linear interpolation may be used to make the equations consistent, e.g.

$$H_\phi^{N+1}(I,J+\tfrac{1}{2}) = \tfrac{1}{2}\left[H_\phi^{N+1}(I,J+1) + H_\phi^{N+1}(I,J)\right] .$$

A close examination of the system will reveal two more inconsistencies which may be treated in the same manner. Upon substitution of the index changes into the system (2.1) - (2.3), the resulting set of equations may be programmed to compute the field components in an iterative manner at suitable time intervals (4).

3 Stability and Convergence

The system of partial differential equations to be solved is a hyperbolic system. For the case where the constitutive properties of the medium are constant, the hyperbolic system has been thoroughly analyzed (3,4,5,6). The resulting difference equations for the hyperbolic system are known to be stable and converge toward the solution provided a restriction is placed on the ratio of grid increments. In general this restriction is that

$$\frac{\Delta\tau}{\Delta z} \equiv \frac{\Delta\tau}{\Delta r} \leq \frac{1}{\sqrt{n}} \tag{3.1}$$

where Δr and Δz are assumed to be equal and n is the number of space dimensions. For the system given in equations (1.8) - (1.10), n=2. It has been found that the best (in terms of economy and accuracy) results are obtained when the time increment to space increment ratio is as large as possible and satisfies the necessary condition given by (3.1). The numerical results presented in the latter part of this chapter were obtained using a grid ratio of 0.5, e.g.

$$\frac{\Delta\tau}{\Delta z} \equiv \frac{\Delta\tau}{\Delta r} = 0.5$$

If the variations in the constitutive properties of the medium are small compared to the variations in the field components, then it may be assumed that the stability and convergence criterion would hold for inhomogeneous and time varying media. It is well known that as the time and space increments approach zero, the solution of the difference equations converges to the exact solution of the partial differential equations.

4 Initial and Boundary Conditions

It is necessary to define the difference equations over a finite region of space. This implies a statement of the appropriate initial and boundary conditions. From Stratton's text (7) a general statement of these necessary conditions may be found:

> An electromagnetic field is uniquely determined within a bounded region V at all times t>0 by the initial values of electric and magnetic vectors throughout V, and the values of the tangential component of the electric vector (or the magnetic vector) over the boundaries for $t \geq 0$.

For convenience, the region under investigation could be considered to be bounded by a perfect conductor so that the appropriate boundary conditions are that the tangential component of the electric field and the normal component of the magnetic field both vanish (8). However instead of posing these conditions, the components on the boundary may be approximated by linear extrapolation. This is the technique which was used to obtain the numerical results given in the next section.

It is necessary to examine the difference equations to determine what boundary conditions are needed over the region. If equation (2.1) is satisfied for I = 1,K and J = 1,L; then (2.2) is satisfied only for I = 1,K and J = 1, L-1, and (2.3) for I = 1, K-1 and J = 1,L. Hence the components which must be determined by extrapolation or boundary conditions are: $E_z^{N+3/2}(I,\tfrac{1}{2})$, $E_z^{N+3/2}(I,K+\tfrac{1}{2})$, $E_r^{N+3/2}(\tfrac{1}{2},J)$ and $E_r^{N+3/2}(L+\tfrac{1}{2},J)$. The first two may be obtained by extrapolation, i.e.

$$E_z^{N+3/2}(I,\tfrac{1}{2}) = 2E_z^{N+3/2}(I,3/2) - E_z^{N+3/2}(I,5/2)$$

$$E_z^{N+3/2}(I,K+\tfrac{1}{2}) = 2E_z^{N+3/2}(I,K-\tfrac{1}{2}) - E_z^{N+3/2}(I,K-3/2)$$

The other two components can be determined by requiring that they equal zero by placing perfectly conducting plates at $z = \frac{\Delta z}{z}$ and $a = (L+\tfrac{1}{2})\Delta z$. The configurations of a cylindrical scatterer and waveguide are shown

in Figure 1. The difference equations are used to determine pulse propagation and scattering from inside a cylindrical waveguide for various shaped scatterers. The electromagnetic boundary conditions at the surface of the scatterer determine certain field components. These components are substituted into the difference equations thereby accounting for the presence of the scatterer. The particular scatterers under consideration are a discontinuous radius cylinder, a cone, and a sphere. The orientations of the respective scatterers in the cylindrical waveguide are shown in Figures 2,3,4. Notice that the surfaces of the cone and the sphere are not coincident with the surfaces formed by the grid points. Hence the boundary conditions for these cases must be approximated in some manner. The technique used in this study is to approximate the boundaries with a "stairstep" type of surface. Then the surfaces of the stairsteps are coincident with the grid surface. Figures 5 and 6 show the longitudinal cross sections of the "approximate" scatterers. The value of certain electromagnetic field components are then known on the approximate surfaces. These values are then imposed on the basic difference equations to account for the shape of the particular scatterer.

Along with the appropriate boundary conditions, it is necessary that the initial components of the fields be known. In this study, the initial components are considered to be those of a pulse propagating in a cylindrical waveguide. These initial fields must

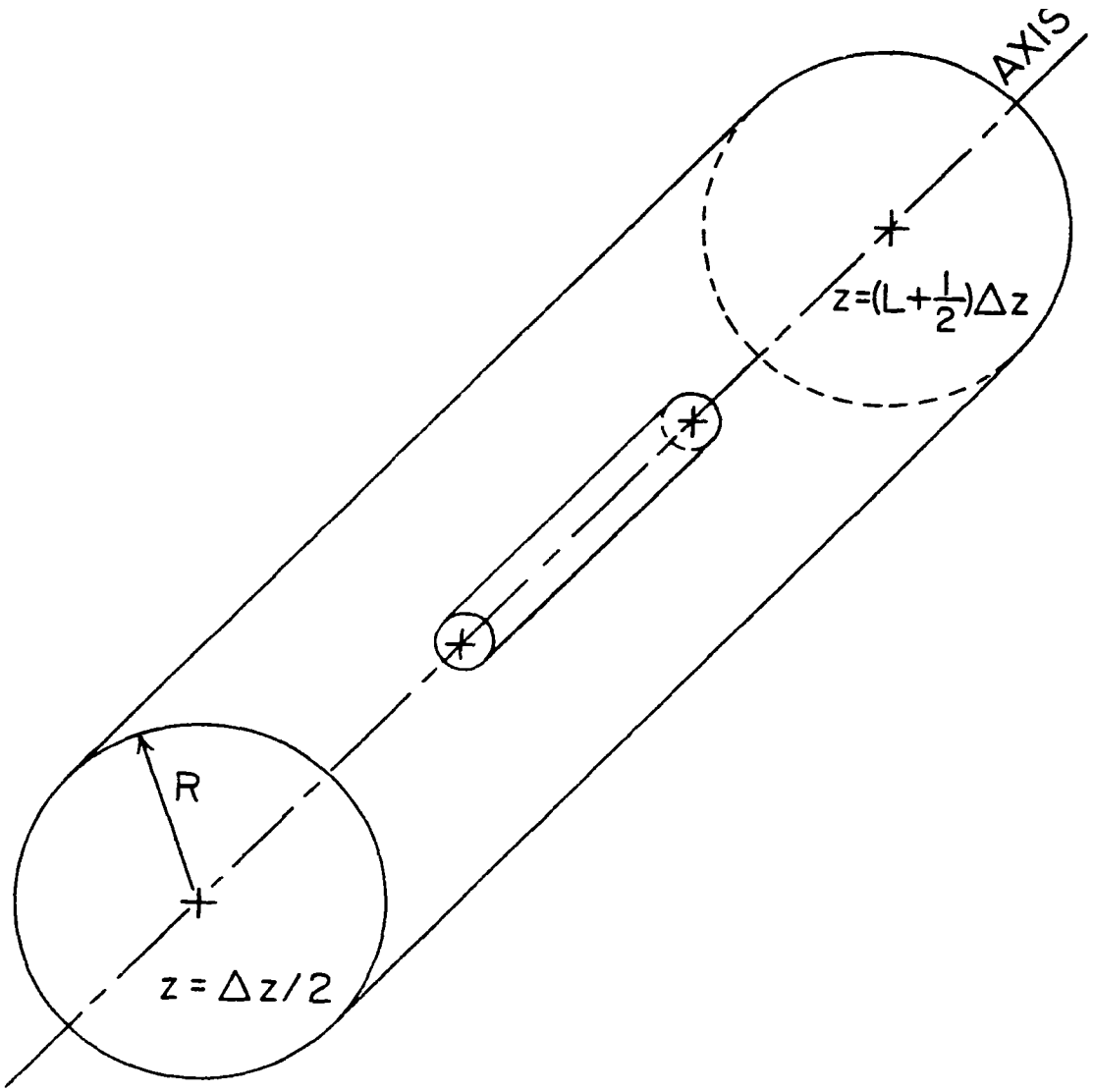

Figure 1 Cylindrical Wave guide containing a solid cylindrical scatterer on axis of the waveguide.

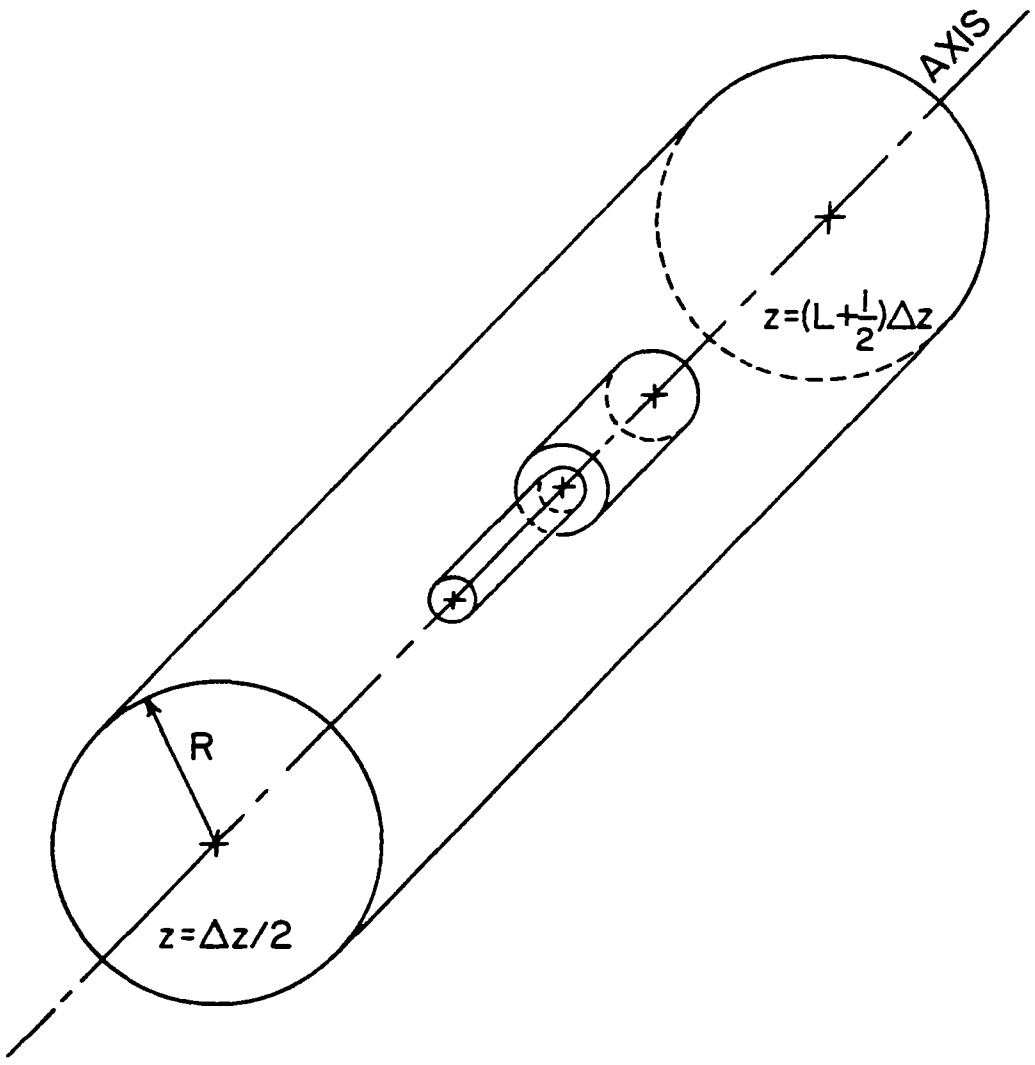

Figure 2 Cylindrical waveguide containing a solid discontinuous radius cylindrical scatterer on axis of the waveguide.

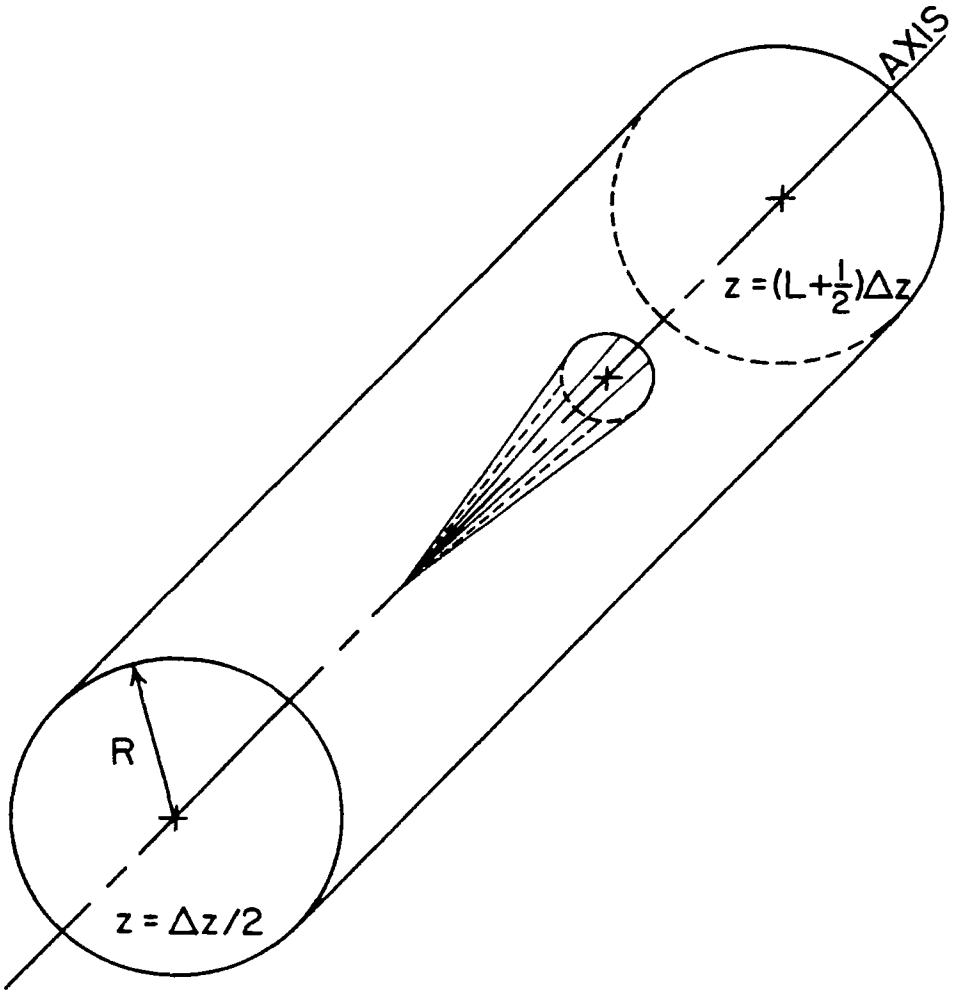

Figure 3 Cylindrical waveguide containing a solid conical scatterer on the axis of the waveguide.

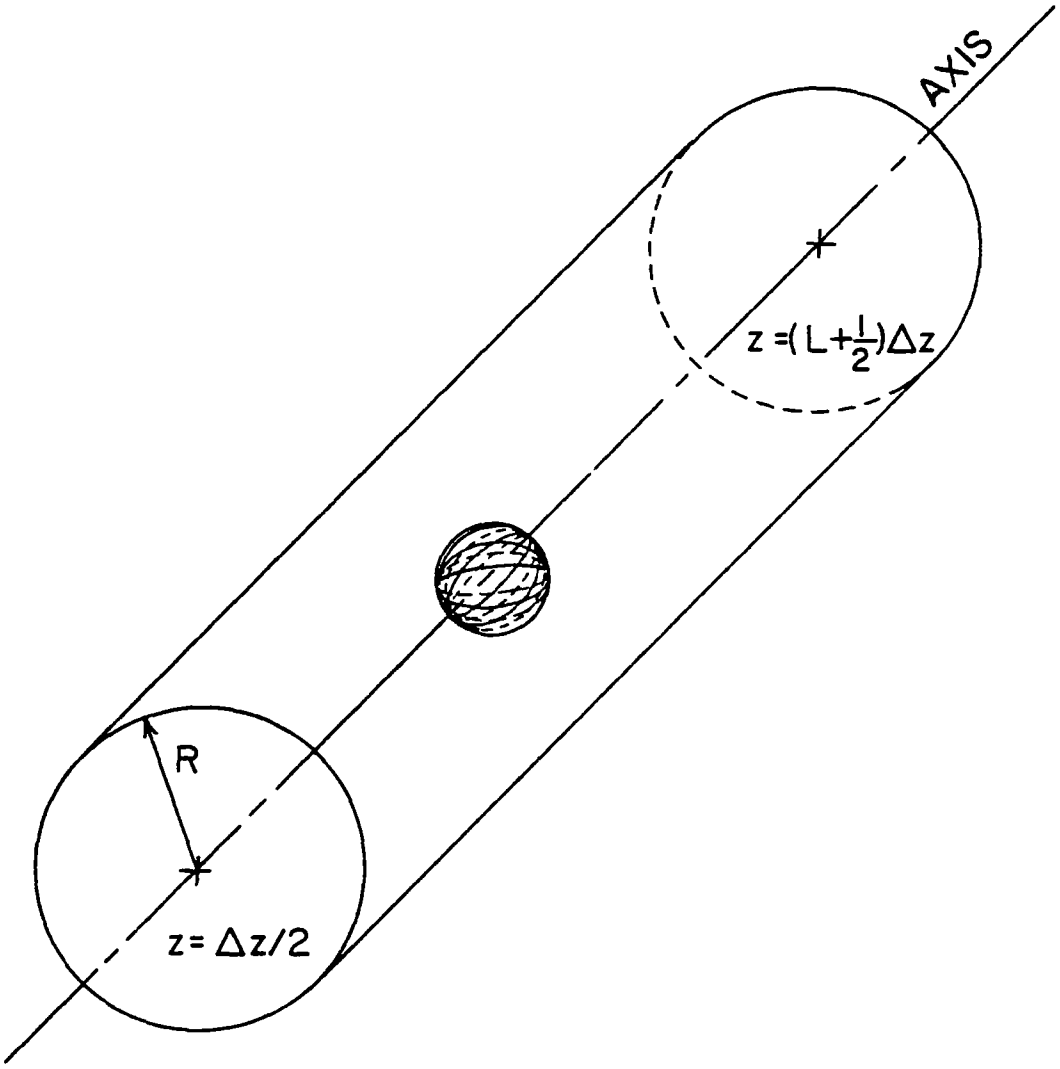

Figure 4 Cylindrical waveguide containing a solid spherical scatterer on the axis of the waveguide.

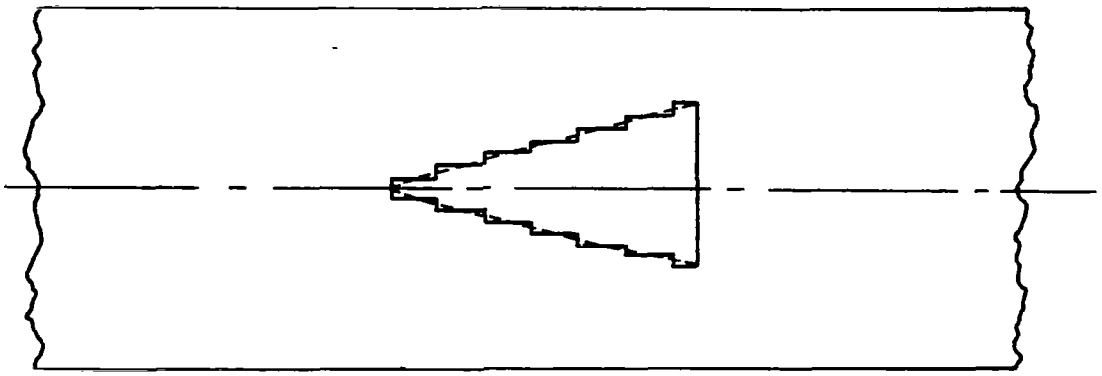

Figure 5 Longitudinal cross-section of cylindrical waveguide and conical scatterer showing the "stairstep" approximation to the surface.

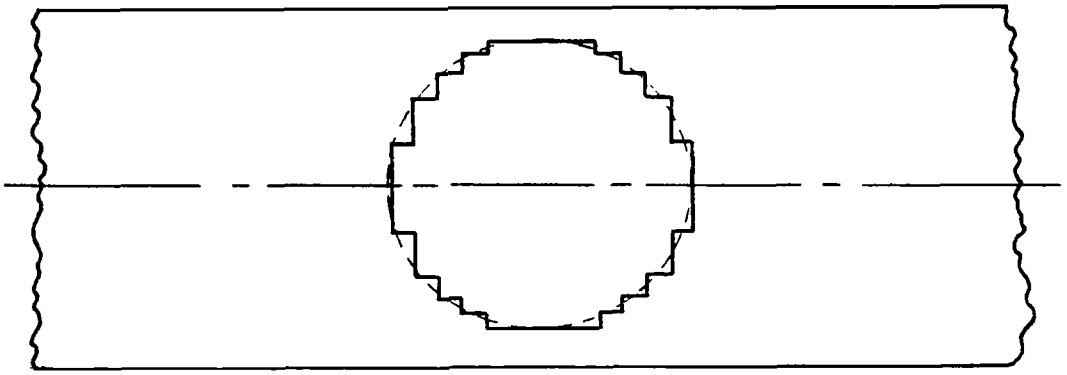

Figure 6 Longitudinal cross-section of cylindrical waveguide and spherical scatterer showing the "stairstep" approximation to the surface.

satisfy certain conditions or restrictions: (1) they must satisfy Maxwell's equations, (2) they must be continuous functions in order for the difference formulas to apply, and (3) they must be axially or rotationally symmetric. For convenience, the initial components of the electromagnetic pulse will be considered to be those of the TM_{01} mode. This is a natural choice since the components of this mode have azimuthal symmetry. The field components of the TM_{01} mode as given by (7) are

$$\tilde{E}_r(z,r,\omega) = j \frac{\beta}{k_c} E_o(\omega) \; J_1(k_c r) \; e^{-j\beta z} \tag{4.1}$$

$$\tilde{E}_z(z,r,\omega) = E_o(\omega) \; J_o(k_c r) \; e^{-j\beta z} \tag{4.2}$$

$$\tilde{H}_\phi(z,r,\omega) = j \frac{k}{\eta_1 k_c} E_o(\omega) \; J_1(k_c r) \; e^{-j\beta z} \tag{4.3}$$

where $E_o(\omega)$ is the complex amplitude of the mode at the radian frequency ω and

$$\beta = \sqrt{k^2 - k_c^2}$$

$$k^2 = \omega^2 \mu_o \varepsilon_1, \qquad \eta_1 = \sqrt{\mu_o/\varepsilon_1}$$

$k_c = 2.405/R$, where R is the radius of the waveguide

The waveguide is assumed to contain a static homogeneous medium with properties μ_o, ε_1, and $\sigma_1 = 0$, although the difference equations are valid for variable constitutive properties provided their initial values are those given above.

The time histories of the field components are expressed as Fourier superpositions of the respective components given by (4.1) - (4.3) . By taking the appropriate derivatives, it can be shown that

$$E_r(z,r,t) = \frac{J_1(k_c r)}{k_c J_o(k_c r)} \frac{\partial}{\partial z} E_z(z,r,t) \tag{4.4}$$

$$H_\phi(z,r,t) = \frac{J_1(k_c r)}{\eta_1 k_c c J_o(k_c r)} \frac{\partial}{\partial t} E_z(z,r,t) \tag{4.5}$$

where

$$E_z(z,r,t) = \frac{J_o(k_c r)}{\sqrt{2\pi}} \int_{-\infty}^{\infty} d\omega \; E_o(\omega) \; e^{-j(\beta z - \omega t)} \tag{4.6}$$

If R is chosen sufficiently large, such that $\beta \simeq k$ for most of the frequency content of the pulse, then equation (4.6) yields

$$E_z(z,r,t) = J_o(k_c r) \; F(z \pm ct) \tag{4.7}$$

where $F(z \pm ct)$ is determined by the choice of $E_o(\omega)$ or vice versa. Because of the restrictions imposed on the initial fields by the finite difference equations, $F(z \pm ct)$ and $F'(z \pm ct)$ must be continuous for all $z \pm ct$, and (4.7) requires that the Fourier transform of $F(z \pm ct)$ must have negligible frequency content for $\omega \leq k_c c$. In this study the choice of $F(z \pm ct)$ subject to the foregoing restrictions is

$$F(z \pm ct) = \begin{cases} \sin^2[A(z \pm ct)] & 0 \leq A(z \pm ct) \leq \pi \\ 0 & \text{elsewhere} \end{cases} \tag{4.8}$$

5 Numerical Results

The numerical results presented here were obtained using an IBM

360 Model 40 computer which carries only 8 significant figures in digital calculations. The radius of the waveguide considered is 2405 meters; each spatial increment, $\Delta z = \Delta r$, is 0.025 meters; and the actual time increment, Δt, is 4.166×10^{-11} sec. The incident electromagnetic pulse field components are those given by (4.4) - (4.8) where

$$A = \pi(18\Delta z)^{-1}$$

and the pulse width at half-maximum is 3/4 nanosecond.

Figure 7 shows the propagation of the axial component of the electric field evaluated at $J = 40$. The pulse is shown at three distinct times; initially, after it has propagated for 25 time increments, and after it has propagated for 50 time increments. Notice that there is a slight disturbance at the tail of the pulse for $N = 50$. This is caused by "round-off" error but has little effect on the results obtained here.

The first scatterer considered is the discontinuous radius cylinder. The total length of the cylinder is 0.350 meters. The discontinuity occurs at the middle of the cylinder with the small radius being 0.050 meters and the large radius being 0.175 meters. In Figure 8, observe the buildup of the current distribution on the surface of the cylinder shown by the solid curve. The two broken curves give a comparison with distributions obtained from continuous cylinders with the same respective radii. These data were taken at the time when the current magnitude was a maximum on the

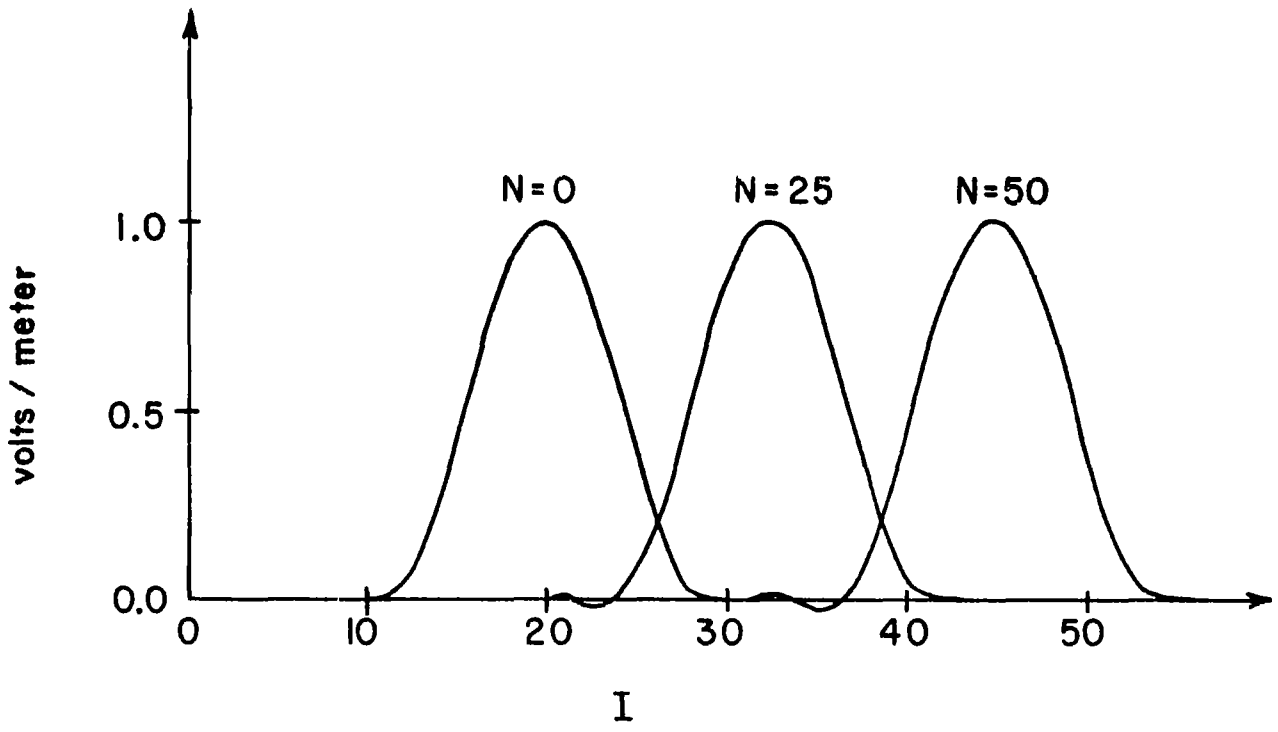

Figure 7 The propagation of the axial component of the electric field evaluated at J = 40. $\Delta z = 0.025$m, $\Delta t = 4.166 \times 10^{-11}$ sec, R = 2405m.

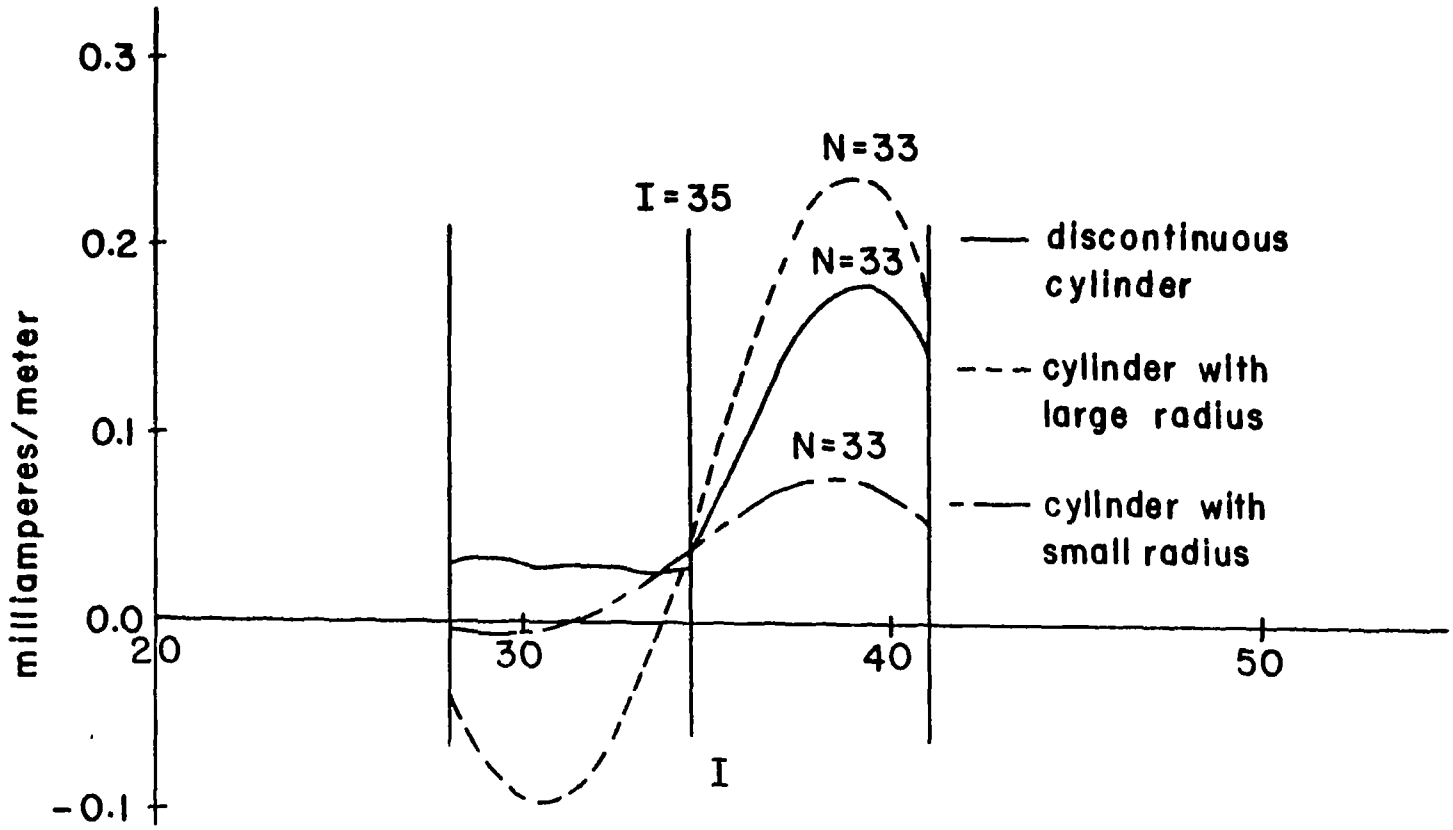

Figure 8 The current distribution induced on the cylindrical scatterer. The peak of the incident pulse at N = 33 is at I = 36. The region of the scatterer is $28 \leq I \leq 42$.

discontinuous-radius cylinder. These same current distributions are shown at a later time in Figure 9. A change in phase is noted as the current is reflected from the end faces of the cylinder.

The second scatterer considered is the cone. Its length is 0.350 meters and its radius at the base 0.175 meters. As indicated before a "stairstep" approximation of the conical surface is used. The current distribution induced on the conical surface is shown in Figure 10. Notice the slight irregularity of the curve. It is expected that a more accurate approximation to the scatterer would produce smoother curves such as those in Figures 8 and 9 where the scattering surfaces are exactly coincident with grid points.

The last numerical data are presented for the sphere with radius of 0.175 meters. Again an approximate surface is used. The current distribution along the surface of the sphere is shown in Figure 11. The slight irregularity in the curve is due to the approximate determination of the boundary conditions of the sphere.

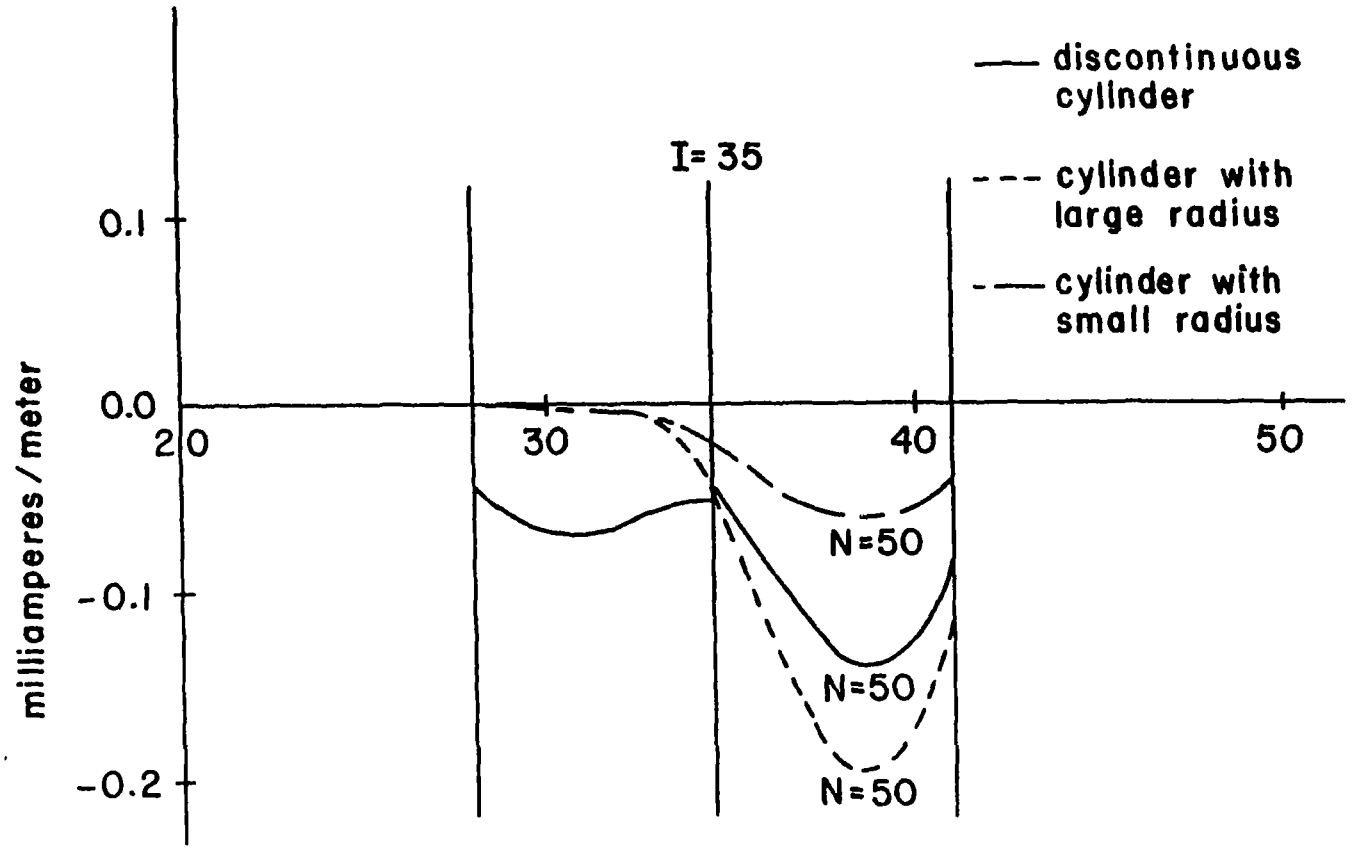

Figure 9 The current distribution induced on the cylindrical scatterer. The peak of the incident pulse at N=50 is at I = 45. The region of the scatterer is $28 \leq I \leq 42$.

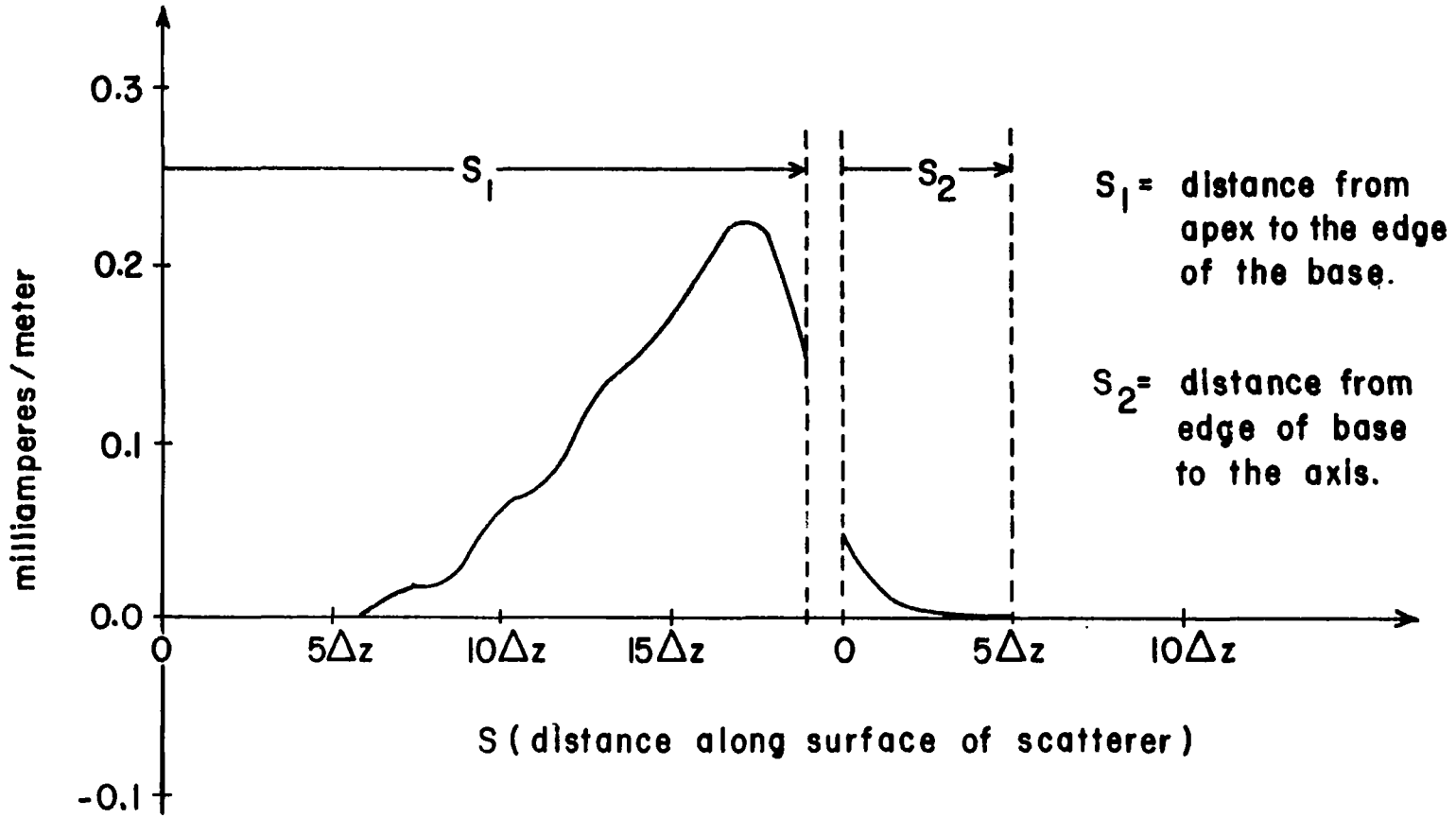

Figure 10 The current distribution induced on the conical scatterer. The peak of the incident pulse at N = 33 is at I = 40. The region of the scatterer is $28 \leq I \leq 42$.

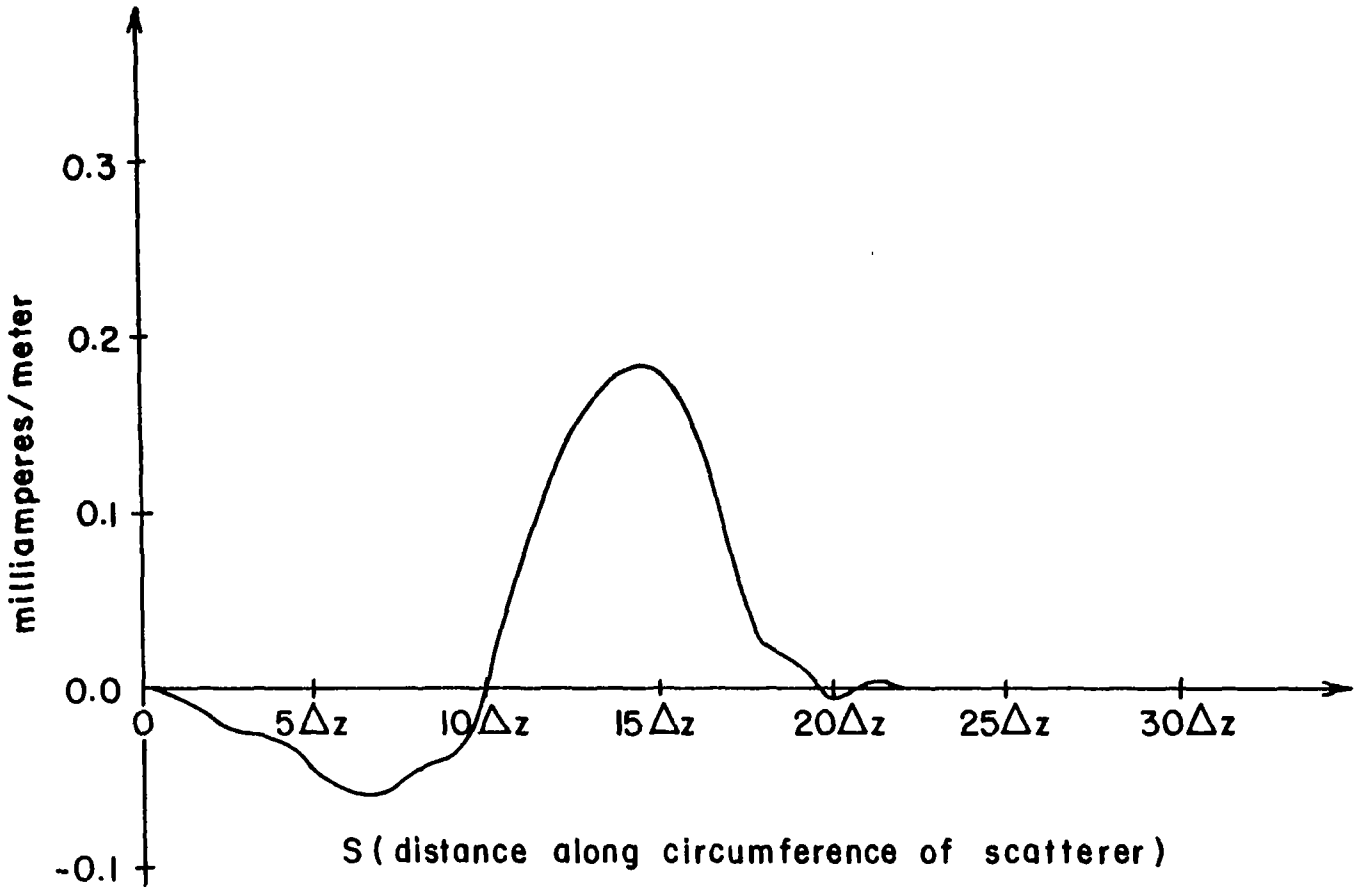

Figure 11 The current distribution induced on the spherical scatterer. The peak of the incident pulse at N = 25 is at I = 35. The region of the scatterer is $28 \leq I \leq 42$.

LIST OF REFERENCES

1. C. D. Taylor, D. H. Lam and T. H. Shumpert, "Two-Dimensional Scattering in Time Varying, Inhomogeneous Media," Interaction Note 41, November, 1968.

2. D. S. Jones, The Theory of Electromagnetism. New York: Pergamon, 1964, p. 3, 5, 10.

3. P. D. Lax, "Differential Equations, Difference Equations and Matrix Theory," Communs. Pure Appl. Math. Vol. 11, pp. 175-194, November 1958.

4. P. Fox, "The Solution of Hyperbolic Partial Differential Equations by Difference Methods," Mathematical Methods for Digital Computers, Edited by A. Ralston and H. S. Wilf, New York: John Wiley, 1964, pp. 180-188.

5. G. E. Forsythe and W. R. Wason, Finite-Difference Methods for Partial Differential Equations. New York: John Wiley, 1960, Section 26.

6. P. D. Lax and R. D. Richtmyer, "Survey of the Stability of Linear Finite Difference Equations," Communs. Pure Appl. Math., Vol. 9, pp. 267-293, September 1956.

7. J. A. Stratton, "Uniqueness of Solution," Electromagnetic Theory, p. 487 (New York: McGraw-Hill, 1941).

8. K. S. Yee, "Numerical Solution of Initial Boundary Value Problems Involving Maxwell's Equations in Isotropic Media," IEEE Trans, Ant. Prop., AP-14, No. 3, pp 302-307, May 1966.